Visual remote sensing image fusion using local correlation moment

Xuhong Yang (杨旭红)[1], Zhongliang Jing (敬忠良)[1], Jianxun Li (李建勋)[1], and Henry Leung[2]

[1] *School of Electrical and Information Engineering, Shanghai Jiaotong University, Shanghai 200030*

[2] *Department of Electrical and Computer Engineering, University of Calgary, Alberta, Canada*

Received April 13, 2004

In this paper a fusion method is proposed for merging a high-resolution panchromatic image and a low-resolution multispectral image. The algorithm is based on discrete wavelet transform (DWT). It uses correlation moment rule to the low frequency bands and local deviation rule to the high frequency bands separately. Experimental results indicate that the proposed approach outperforms the traditional methods.

OCIS codes: 350.2660, 100.7410, 110.3000, 100.2980.

In the last two decades the plethora of the multi-sensor and multi-temporal remote sensing data highlighted the needs for a meaningful combination of all employed imaging sources. Image fusion of high spatial resolution data and multi-spectral data gives a hybrid image with good terrain details and useful spectral information, which in turn can discriminate small objects or land cover types. A number of methods have been proposed for merging panchromatic and multi-spectral data such as: intensity-hue-saturation (IHS) method[1], principal component analysis (PCA) method[2] and high-pass filter (HPF)[3] method. All these techniques strongly enhance textural features but they also cause significant spectral degradation. Recently, several authors proposed a new approach to image merging that uses a multi-resolution analysis procedure based upon the discrete two-dimensional (2D) wavelet transform[4−6]. The wavelet transform provides a framework to decompose images into a number of new images, each one of them with a different degree of resolution, and it can provide good localization in both frequency and space domains. After wavelet decomposition, couples of sub-bands of corresponding frequency content are merged and the fused image is synthesized by taking the inverse transform.

The quality of the fused image is determined by the fusion rules taken in the process of merging. The fusion rules include pixel-based rules and window-based rules. Pixel-based rule selects the maximum of the absolute value of corresponding pixels. One of the window-based rules is based on the local standard deviation, that is: on 2^j resolution level, if the standard deviation estimated from local neighborhoods of a pixel in image A is not less than in image B, then the fused wavelet coefficients of this pixel are assigned as the wavelet coefficients of image A; otherwise, the fused wavelet coefficients of this pixel are assigned as the wavelet coefficients of image B.

In the fusion process, using the pixel-based rules in the selection of wavelet coefficients may induce error coefficients selection so the fusion result may be affected by the isolated noise point. On the contrary, when window-based rules are used in the selection of wavelet coefficients, the selection is based on the whole information of the local windows. So the independent information of each pixel is not taken into account.

In 2002, a multi-resolution wavelet decomposition fusion algorithm based on local correlation moment rule is proposed[7]. In this paper, it is stated that local correlation moment rule performs well in improving the spatial resolution of the multi-spectral imagery.

The local correlation moment is defined as

$$M_{ij}^{k} = \left| \frac{\varpi_{ij} - \mu_j}{\sigma_j} \right|, \tag{1}$$

where ϖ_{ij} is the wavelet decomposition coefficient of the i pixel in the j window, μ_j is the standard deviation of the wavelet decomposition coefficients in the j window, and $k = 1, 2, 3$ denotes that the coefficients are of horizontal high frequency component, vertical component and diagonal high frequency component, respectively.

The local correlation moment rule can be stated as follow: if the correlation moment calculated from local neighborhoods of a pixel in image A is not less than in image B, then the fused wavelet coefficients of this pixel are assigned as the wavelet coefficients of image A; otherwise, the fused wavelet coefficients of this pixel are assigned as the wavelet coefficients of image B.

The virtues of the fusion rules based on the local correlation moment are as below. The local correlation moment takes the both the local mean and standard deviation into account. This model is based on every decomposition coefficient in the local window other than takes the whole window as a object to process, so it can make full use of the ability of wavelet to decompose images into different frequency bands. Multi-resolution analysis can be used for selecting local window to get local correlation moment in order to utilize the multi-resolution analysis characteristic of wavelet.

In this paper, three evaluation criteria are used for quantitatively assessing the performance of the fusion results.

1) the average gradient (AG) of the image

The average gradient reflects the clarity of an image. It can be used to measure the spatial resolution of the fused image. A larger average gradient means better spatial resolution

$$\mathrm{AG} = \frac{1}{(M-1)(N-1)} \sum_{x=1}^{(M-1)} \sum_{y=1}^{(N-1)} \sqrt{\left[\left(\frac{\partial f(x,y)}{\partial x}\right)^2 + \left(\frac{\partial f(x,y)}{\partial y}\right)^2\right]/2}. \quad (2)$$

2) mutual information (MI)[8]

MI represents how much information has been obtained from the fusion of input images. The equation of calculating MI is given as

$$\mathrm{MI} = \sum_{i=1}^{L}\sum_{j=1}^{L} h_{\mathrm{R,F}}(i,j) \log_2 \frac{h_{\mathrm{R,F}}(i,j)}{h_{\mathrm{R}}(i) h_{\mathrm{F}}(j)}. \quad (3)$$

where $h_{\mathrm{R,F}}(i,j)$ is the joint histogram of images R and F, $h_{\mathrm{R}}(i)$ and $h_{\mathrm{F}}(j)$ are the marginal histogram distributions of the source images R and F, respectively, L is the degree of intensity. MI is used to evaluate the spectral fidelity of fused image. Large MI implies better image quality.

3) correlation coefficients (CORR)

$$\mathrm{CORR}(A,B) = \frac{\sum_{i,j}^{N} [(A_{i,j} - \overline{A}) \times (B_{i,j} - \overline{B})]}{\sqrt{\sum_{i,j}^{N} [(A_{i,j} - \overline{A})^2] \times \sum_{i,j}^{N} [(B_{i,j} - \overline{B})^2]}}, \quad (4)$$

where $\overline{A}$ is the average intensity of image A and $\overline{B}$ is the average intensity of image B. Correlation coefficients are used to measure the similarity of two images. A large correlation coefficient means better spectral fidelity.

Our research includes 3 parts: 1) the different effects of local correlation moment rule on low frequency band and high frequency band; 2) the influence of the size of the local windows on the fusion results; 3) the comparison of the proposed fusion algorithm to the fusion algorithms of pixel-based rules and window-based rules.

In order to study the different effects of local correlation moment rule on low frequency band and high frequency band, local correlation moment rule is used on low frequency band and high frequency band separately. The fusion results are also compared with the fusion results of pixel-based rule and local standard deviation rule.

The conclusion of experiment is quite different from Ref. [5]: local correlation moment rule performs best in the protection of local spectral information while local standard deviation rule gets the best result in spatial enhancement. The conclusion can be explained as below: high-resolution panchromatic images have plenty detail information of texture included in high frequency component, while multi-spectral images have an abundance of spectral information centralized in low frequency component. According to the analysis of frequency characteristics of the different kind images from same area, the low frequency components of images are similar but the high frequency components are quite different. Taking local standard deviation rule in merging low frequency component really means taking the local window as a single merging object. It causes insufficient revealing of the difference between the low frequency components of the two images. So the spectral information is not well preserved. On the contrary, adopting local correlation moment rule gives prominence to the independent information of each pixel, but it is not as good as local standard deviation rule in considering the continuity of texture information and protecting texture information of a little big size in images.

Another important conclusion has been drawn in the process of studying the influence of the window size on the fusion result. It is described in details as following: only in the level one of decomposition, the size of the window in merging has the effect on the fusion result; while the size of merging windows in other levels of decomposition has no effect on the fusion result.

Figure 1 illustrates influence of the size of local windows in the first level of decomposition on the fusion result. From Fig. 1, it can be seen clearly that window of the size of 3×3 leads to the best merging result for our fusion algorithm.

Now the proposed fusion algorithm (local correlation moment deviation (LCMD) for short) is stated in details: using local correlation moment rule to the low frequency part and local standard deviation rule to the high frequency part. The proposed method is used to merge QuickBird 0.7-m panchromatic image and the corresponding QuickBird 2.8-m multi-spectral image of the Shanghai area, acquired on 2002. The size of image is 512*512. The low-resolution multi-spectral image and the high-resolution panchromatic image are from the same sensor and not need any register.

The steps of this fusion method to perform are described in detail as following.

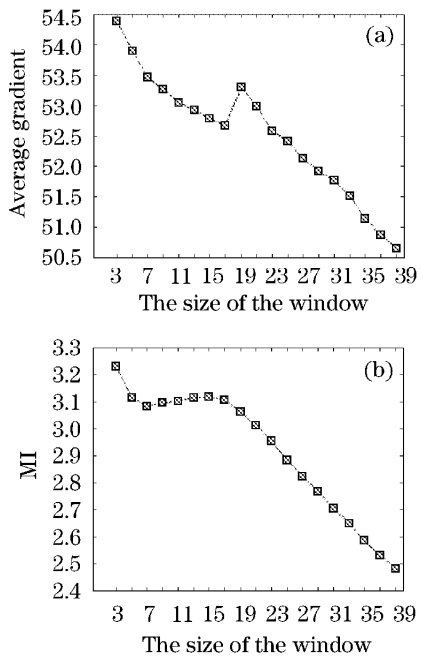

Fig. 1. The effect of window size on the evaluation criteria. (a) The curve of average gradient verifies with the size of window; (b) the curve of MI verifies with the size of window.

1) Transform the R, G, and B bands of the multi-spectral image into the IHS components as following

$$\begin{bmatrix} I \\ V_1 \\ V_2 \end{bmatrix} = \begin{bmatrix} 1/3 & 1/3 & 1/3 \\ 1/\sqrt{6} & 1/\sqrt{6} & -2/\sqrt{6} \\ 1/\sqrt{2} & -1/\sqrt{2} & 0 \end{bmatrix} \begin{bmatrix} R \\ G \\ B \end{bmatrix}, \quad (5)$$

where $H = \tan^{-1}(V_2/V_1)$, $S = \sqrt{V_1^2 + V_2^2}$; I is the intensity, H is the hue, S is the saturation, and V_1, V_2 are the intermediate variables.

2) Perform conventional histogram matching between the panchromatic image and the intensity component of the IHS representation. Specifically, after computing the histogram of both the panchromatic image and the intensity component of the multi-spectral image, the histogram of the intensity of the multi-spectral is used as reference to which we match the histogram of the panchromatic image.

3) The intensity component of the multi-spectral image and the panchromatic image are decomposed into a wavelet representation at the same coarser resolution. In our algorithm, we let decomposition level $n = 3$. Couples of sub-bands of corresponding frequency content are merged using LCMD algorithm. The fused image is got by inverse wavelet transform (IDWT).

4) The inversed IHS transformation is performed to get the merged RGB image with merged high-resolution information.

The algorithms of the pixel-based rule and the local standard deviation rule are used in comparing the performance of the presented algorithm. Two groups of panchromatic images and the corresponding multi-spectral images are used in our research.

Figures 2(a) and (b) are the first group of images of QuickBird 0.7-m panchromatic image and the corresponding 2.8-m multi-spectral image. Fusion results by using different fusion rules are shown in Figs. 2(c)−(e), respectively.

Figures 3(a) and (b) show the second group of images of QuickBird 0.7-m panchromatic image and the corresponding 2.8-m multi-spectral image. Fusion results by using different fusion rules are given in Figs. 3(c)−(e), respectively.

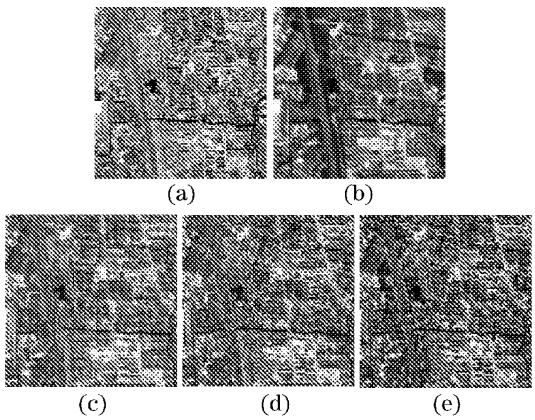

Fig. 2. The original images and fusion images of the first group of data. (a) The original QuickBird 0.7-m image; (b) the original QuickBird 2.8-m image; (c) fusion image of pixel-based rule; (d) fusion image of local standard deviation rule; (e) fusion image of LCMD algorithm.

Figures 4(a) and (b) show the third group of images of QuickBird 0.7-m panchromatic image and the corresponding 2.8-m multi-spectral image. Fusion results

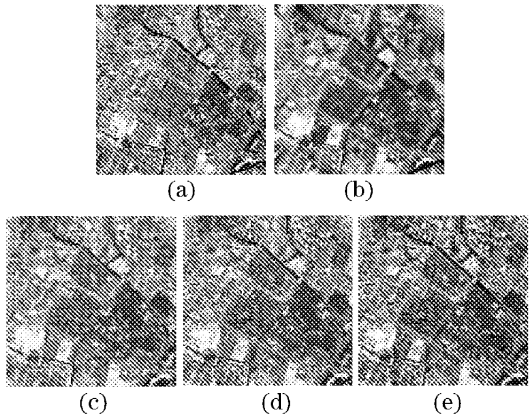

Fig. 3. The original images and fusion images of the second group of data. (a) The original QuickBird 0.7-m image; (b) the original QuickBird 2.8-m image; (c) fusion image of pixel-based rule; (d) fusion image of local standard deviation rule; (e) fusion image of LCMD algorithm.

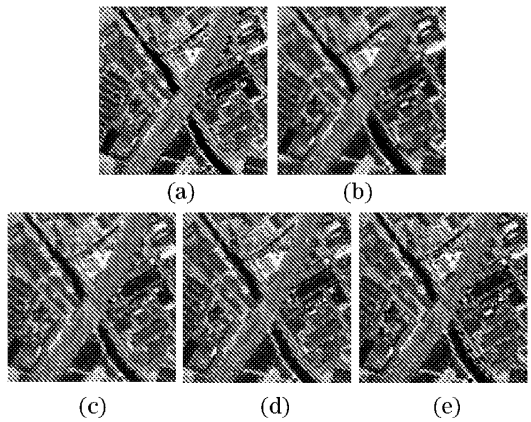

Fig. 4. The original images and fusion images of the third group of data. (a) The original QuickBird 0.7-m image; (b) the original QuickBird 2.8-m image; (c) fusion image of pixel-based rule; (d) fusion image of local standard deviation rule; (e) fusion image of LCMD algorithm.

Table 1. Evaluation Results of the 1st Group Images

Image Data	Tunnel	AG	CORR	MI
Fig. 2(b)	R	8.2997	/	/
	G	8.0616	/	/
	B	7.3599	/	/
Fig. 2(c)	R	21.295	0.7741	1.1779
	G	21.279	0.757	
	B	21.01	0.7284	
Fig. 2(d)	R	25.16	0.6867	1.5989
	G	25.235	0.671	
	B	25.013	0.6433	
Fig. 2(e)	R	25.896	0.7012	1.6279
	G	25.964	0.6823	
	B	25.738	0.6496	

Table 2. Evaluation Results of the 2nd Group Images

Image Data	Tunnel	AG	CORR	MI
Fig. 3(b)	R	8.7551	/	/
	G	8.6081	/	/
	B	7.9421	/	/
Fig. 3(c)	R	22.316	0.7011	1.5605
	G	22.247	0.6823	
	B	22.002	0.6496	
Fig. 3(d)	R	26.21	0.7714	2.114
	G	26.125	0.7809	
	B	25.989	0.7598	
Fig. 3(e)	R	26.693	0.7803	2.1905
	G	26.642	0.7871	
	B	26.463	0.7671	

Table 3. Evaluation Results of the 3rd Group Images

Image Data	Tunnel	AG	CORR	MI
Fig. 4(b)	R	5.655	/	/
	G	5.6873	/	/
	B	5.3898	/	/
Fig. 4(c)	R	11.717	0.9118	2.3186
	G	11.706	0.9098	
	B	11.58	0.9017	
Fig. 4(d)	R	12.704	0.8747	2.7369
	G	12.685	0.8724	
	B	12.598	0.8609	
Fig. 4(e)	R	13.071	0.8809	2.8699
	G	13.047	0.8772	
	B	12.952	0.8657	

by using different fusion rules are given in Figs. 4(c)−(e), respectively.

It can be seen in Figs. 2−4 that the fusion results of LCMD algorithm are better than pixel-based rule and local standard deviation rule in spectral information protection as well as spatial resolution enhancement.

Tables 1−3 show evaluation results (average gradients, correlation coefficient and MI) of the fused images from various methods. The LCMD algorithm produces the biggest average gradient and MI than other methods.

Three important conclusions are stated as below. The local correlation moment rule performs better in spectral fidelity but is poor in spatial enhancement comparing with local standard deviation rule; only on the level one of wavelet decomposition, the size of the window used in merging has influences on the fusion result; comparing with the traditional method, the LCMD algorithm can efficiently preserve the spectral information and improve the spatial resolution of remote sensing images by using local correlation moment rule to the low frequency bands and local standard deviation rule to the high frequency bands.

This work was jointly supported by the National Natural Science Foundation of China (No. 60375008), China National '863' Project (No.2001AA135091), Shanghai Key Scientific Project (No. 02DZ15001), Aviation Science Foundation (No. 02D57003), and China Ph.D Discipline Special Foundation (No. 20020248029). X. Yang's e-mail address is yxh@sjtu.edu.cn.

References

1. C. C. Teoh, S. B. Mansor, M. R. Mispan, A. R. Mohamed Shariff, and N. Ahmad, in *Proceedings of IGARSS'01* **3,** 1490 (2001).
2. J. M. Piwowar and A. A. Millward, in *Proceedings of IGARSS'02* **3,** 1851 (2002).
3. J. G. Liu, International J. Remote Sensing **21,** 3461 (2000).
4. R. L. King and J. W. Wang, in *Proceedings of IGARSS'01* **2,** 849 (2001).
5. P. Scheunders, IEEE Trans. Image Processing **12,** 718 (2003).
6. Y. Chibani and A. Houacine, in *Proceedings of The 7th IEEE International Conference on Electronics, Circuits and Systems* **1,** 442 (2000).
7. Y. F. Gu, Y. Zhang, and J. P. Zhang, in *Proceedings of International Conference on Image Processing* **2,** 357 (2002).
8. G. H. Qu, D. L. Zhang, and P. F. Yan, Electron. Lett. **38,** 313 (2002).